W. Rodi
Professor,
Institut für Hydromechanik,
Universität Karlsruhe,
Karlsruhe, Germany

J. H. Ferziger
Professor,
Department of Mechanical Engineering,
Stanford University Stanford, CA 94305-3030

M. Breuer
Researcher.

M. Pourquié
Researcher.

Institut für Hydromechanik,
Universität Karlsruhe,
Karlsruhe, Germany

Status of Large Eddy Simulation: Results of a Workshop

1 Introduction

The mixed quality of the results obtained with conventional (Reynolds averaged) turbulence models i.e., those used in conjunction with the Reynolds averaged Navier-Stokes or RANS equations, together with the continually decreasing cost of doing computations, has led to increased interest in the possibility of using large eddy simulation (LES) as a tool for prediction of practical turbulent flows. This paper is, in large part, a summary of the results presented at a conference designed to assess the current state of the art in LES for complex flows and the conclusions reached on the basis of those results.

Large eddy simulation was first applied to engineering flows by Deardorff (1970). In the early days, its application was limited to simple flows and to a small number of groups fortunate enough to have access to supercomputers. In essence, it was developed to complement laboratory experiments in the investigation of the fundamental processes that occur in relatively simple turbulent flows. When the capability of computers increased still further in the 1980s, it became possible to perform direct numerical simulations (DNS) of interesting flows and the latter became the preferred approach to fundamental studies of turbulence. More recently, the possibility of simulating more complex flows has reawakened interest in LES; interest centers on flows too difficult to treat with DNS, mainly ones in complex geometries. The decreasing cost of computing has also put the possibility of using LES into the hands of many more people.

The success that LES has had is, in the opinion of the authors, largely due to careful selection of target flows and the parameters used in the simulations. There is a danger that this success may give some people the impression that success is automatic and thus lead to over-optimism that LES is bound to be successful. This impression is, of course, not correct; a great deal of research is required before it will be known how widely the method can be used.

Contributed by the Fluids Engineering Division for publication in the JOURNAL OF FLUIDS ENGINEERING. Manuscript received by the Fluids Engineering Division July 10, 1996; revised manuscript received January 2, 1997. Associate Technical Editor: S. P. Vanka

As with any method, there is a need for continuous assessment of the models, numerical methods, and geometrical treatments that are used in LES of complex flows. It is time to begin to perform such assessments. It was for precisely this reason that the authors coordinated a workshop designed to assess the present state of the art in LES of complex flows (Workshop on Large Eddy Simulation of Flows past Bluff Bodies). It was held in Rottach-Egern, Germany on 26–28 June 1995. The participants, all of whom were required to submit results of simulations, are listed in Tables 3, 5, and 6.

In the remainder of this paper we shall present a short overview of LES, the subgrid scale models that are used in LES, the numerical methods used, results obtained for two complex flows, and an assessment of those results.

2 A Short Overview of LES

The methods and models used in large eddy simulation have been presented in many papers. It is traditional in such papers to present the equations anew each time but, by now, the fundamental equations that are solved in LES should be familiar to most readers, making another presentation of them unnecessary. Accordingly, we shall break with tradition and not write the detailed equations here. Rather, a short description of them will be given. The reader desiring an introduction to the practice of LES is referred to articles by Ferziger (1983), Moin and Rogallo (1984), Ferziger (1996), and Breuer et al. (1996a, 1996b).

The objective of large eddy simulation is to explicitly simulate the large scales of a turbulent flow while modeling the small scales. To do so, one begins by filtering the Navier-Stokes equations to obtain an equation for the large scale motions. As stated above, these equations, which have been given in the literature many times, will not be presented here. The most important point is that the nonlinearity of the Navier-Stokes equations makes it impossible to obtain an exact closed equation for any filtered quantity. This means that a term analogous to the Reynolds stress in RANS is produced and must be modeled. For incompressible flow, the density may be normalized out and the quantity to be modeled is:

$$\tau_{ij} = \overline{u_i u_j} - \overline{u}_i \overline{u}_j \tag{1}$$

An overbarred quantity is one that has been filtered. The

quantity τ_{ij} defined by Eq. (1) is called, naturally enough, the subgrid scale Reynolds stress. It represents the interactions between the large scales that we intend to simulate and the small scales that have been filtered away. In the absence of information about the small scales, an exact expression for this term is impossible to construct so models, called subgrid scale (SGS) models, are required. These are described in the following section of this paper.

It is also important to note that the filtered Navier-Stokes equations must be solved accurately in both space and time. Filtering removes the smallest scales but, in the desire to obtain the most from a simulation, one usually tries to retain as much energy in the resolved scales as possible. To accomplish this, it is necessary to leave considerable energy in the smallest resolved scales. This places a heavy demand on the accuracy of the spatial discretization method and usually means that the order of a discretization approximation is not a good measure of its accuracy. It also makes LES prone to errors that produce wiggles in the solution and aliasing errors; the latter may make a simulation unstable. Many of the simulation results presented at the conference exhibit at least a small bit of wiggly behavior, indicating that they have not used sufficient resolution.

Upwind methods are often employed to eliminate the wiggles that central difference methods are prone to produce. They accomplish this by introducing diffusion (often of order higher than two), thereby producing a smooth field. When used with sufficient resolution, upwind methods are capable of producing results as accurate as central difference methods. However, the added viscosity should be counted as part of the model and its contribution to the dissipation of energy should be measured; estimation of the effect of numerics on energy dissipation was not required in the workshop discussed herein.

3 Models

3.1 Subgrid Scale (SGS) Models. In this section we shall introduce the subgrid scale models used in the simulations. The nature of this paper demands that we sacrifice completeness in order to introduce only the models that were applied by the conference participants. We shall try to stick to this script and be as brief as possible without trivializing the subject.

By far the oldest and best known subgrid scale model is the one due to Smagorinsky (1963). It can be considered the large eddy simulation version of the well-known mixing length model of Prandtl and can be written:

$$\tau_{ij} = -2\nu_T \bar{S}_{ij} \tag{2}$$

where ν_T is the eddy viscosity and $\bar{S}_{ij}$ is the strain rate in the resolved velocity field. By dimensional analysis, one can demonstrate that a reasonable form for the eddy viscosity is:

$$\nu_T = (C_S\Delta)^2 |\bar{S}| \tag{3}$$

where $|\bar{S}|^2 = \bar{S}_{ij}\bar{S}_{ij}$ and Δ is the length scale associated with the filter i.e. it is the length that distinguishes a 'small' eddy from a "large" one. The parameter in this expression can be computed from various theories which suggest that, for isotropic turbulence:

$$C_S \approx 0.2 \tag{4}$$

This model (with different values of the parameter) was in fact used by approximately half the participants at the conference that is the subject of this paper.

Despite its usefulness, the Smagorinsky model has significant disadvantages. It has long been known that, to obtain the proper behavior in a region close to a wall, it is necessary to introduce a rather arbitrary damping of the eddy viscosity produced by the Smagorinsky model. This modification is difficult to justify and hard to apply in complex geometries. The eddy viscosity also needs to be reduced when stratification and/or rotational effects are present. In regions of anisotropic turbulence (which require anisotropic filters), the choice of length scale is not obvious. Finally, the Smagorinsky model is not capable of predicting laminar-turbulent transition in wall-bounded flows accurately because it dissipates too much energy too early in the simulated flow.

To improve on the Smagorinsky model one can follow the direction long used in RANS modeling and introduce one or more partial differential equations for the quantities that determine the model. This approach has been used a few times but has not met with great success. An approach that has had more success is to use the small scales of the resolved field to determine the model for the unresolved scales. One such model is the scale-similarity model of Bardina et al. (1981), which in the form most commonly used today, is:

$$\tau_{ij} = \overline{\bar{u}_i\bar{u}_j} - \bar{\bar{u}}_i\bar{\bar{u}}_j \tag{5}$$

where the double overbar means that the quantity has been filtered twice. (Double filtering gives a smoother result than single filtering.) This model does not dissipate much energy and must be combined with the Smagorinsky model to be useful. The resulting mixed model has been used quite often and with considerable success.

The final approach to be discussed in this section is not really a model at all but is better called a procedure. This is the dynamic method of Germano et al. (1991). We shall not present full details of this procedure here; only an outline is given. The interested reader is referred to the original papers for complete details. In the dynamic procedure, one uses the smallest scales of the resolved field to determine the parameters of the model. By filtering the velocity field with a filter wider than the one used in the LES one can make a kind of a priori test (Clark et al., 1979) to determine the model parameter. In the simplest version of the method, the Smagorinsky model is assumed to hold on both the original LES level and the 'test filter' level. By using an identity given by Germano et al. (1991), it is possible to find a set of equations for the parameter. In fact, there are five equations for the single parameter and they can only be satisfied in the least squares sense, an approach first suggested by Lilly (1992). The result of the dynamic procedure is a value of the model parameter that varies with position and time, sometimes in quite dramatic fashion.

The dynamic procedure with the Smagorinsky model as the base model produces large negative eddy viscosities that can make a simulation numerically unstable. A number of cures for this problem have been suggested. One is to average some of the quantities over one or more homogeneous coordinate directions (done originally by Germano et al., 1991) or time (Piomelli, 1992). Another is to simply replace any negative eddy viscosity by zero (clipping). A third is to replace the Smagorinsky model, using the mixed model as the base model; this was used (with pre-filtering to remove potential problems caused by the small scales) in one submission to the conference. All of these help in mitigating the instability but none has yet proven completely satisfactory.

3.2 Wall Models. In wall bounded flows, the only correct boundary condition at the surface is the no-slip condition. However, the turbulent flows develop very small structures near walls; this has been well-documented. As the ratio of the thickness of the viscous sublayer to the overall boundary layer decreases with Reynolds number, the problem becomes worse at high Re. These structures play a very important role in the production of turbulence and thus in determining the skin friction but resolving them is very expensive due to the large number of grid points that must be used. It would be useful to have a way to avoid the necessity of resolving them.

One can apply an artificial boundary condition at some distance from the wall. In a fully developed equilibrium flow, the logarithmic region is an obvious place to try this approach. A

number of conditions that can satisfactorily represent this region for equilibrium flows have been developed. They are designed to force the mean velocity profile to have the proper logarithmic behavior in this region. Most of these were not used in the simulations discussed in this paper so we shall not review them; the interested reader is referred to the paper of Piomelli et al. (1989). A generalized condition that allows the location at which the condition is applied to lie below the logarithmic region was given by Werner and Wengle (1989); it is based on a power law profile that is capable of giving an approximate representation of the instantaneous velocity profile throughout the inner region of the boundary layer. This condition was used in a number of the submitted simulations.

When the Reynolds number is very large, the logarithmic region and viscous sublayer cover a very small part of the boundary layer and the grid used in the simulation may be sufficiently large that the filtering process removes much of the fluctuating component of the velocity. If the boundary layer is of equilibrium type, it is reasonable to require that the instantaneous velocity profile be logarithmic. A condition of this type was suggested by Mason (1992) and is often used in LES of the atmospheric boundary layer, where it seems to perform reasonably well. This corresponds to a kind of very large eddy simulation but it is doubtful that many engineering flows qualify for such treatment. For reviews of LES of the atmospheric boundary layer, see Nieuwstadt et al. (1993) and Andren et al. (1994).

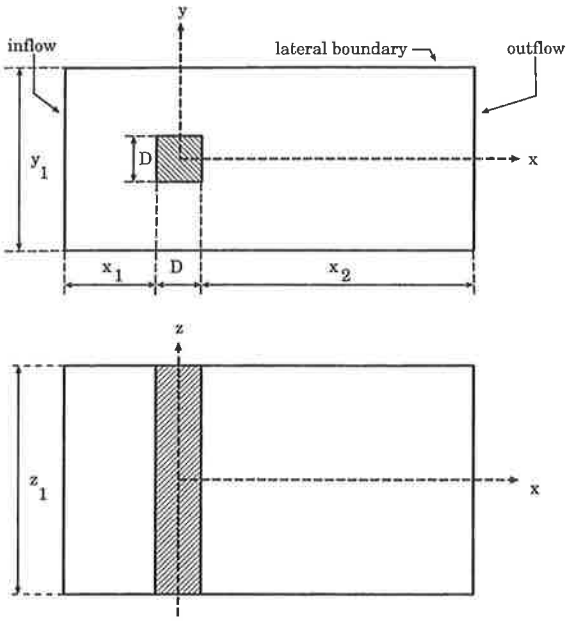

Fig. 1 The geometry of the square cylinder flow (Test Case A) indicating the definitions of the various geometric lengths

4 The Test Cases

In the past, large eddy simulation has been applied mainly to relatively simple flows including essentially all possible variations of homogeneous turbulence, simple free shear flows, channel flow, and boundary layers (including the atmospheric boundary layer), to mention a few. Most of these flows can also be treated with direct numerical simulation, at least at low enough Reynolds numbers. There have been a few attempts at simulation of complex flows with LES but they involved flows for which the results are difficult to verify in detail so we shall not say more about them here.

The ideal flows for application of LES would have the following properties:

- The Reynolds numbers should be high enough to be out of reach of DNS but not so high that the model is the dominant factor in the simulation.
- The geometry should be complex enough to render DNS infeasible but not so complex that the number of grid points needed for accurate representation of the geometry is too high.
- The physics of the flow should be relatively complex. At minimum, the flow should contain significant secondary flows, separation, or other 'extra strains' that make modeling with Reynolds averaged models difficult.
- Reliable and complete experimental measurements of the flow should exist.

In choosing test cases for the conference, we were guided by the above criteria. Since this was the first conference of this kind (the conference reported in Voke et al. (1994) was of a somewhat different type), in order to avoid having too few participants due to difficulties in generating adequate grids, we added the further constraint that the geometries should be ones for which gridding is relatively easy. In practice, we restricted our attention to flows for which the geometry could be treated with a Cartesian coordinate system.

The first case selected (designated Case A) was the flow over a square cylinder for which measurements were reported by Lyn and Rodi (1994) and Lyn et al. (1995). The Reynolds number was 22,000 and the inflow was reported to have a turbulence level of 2 percent at 4.5 cylinder widths upstream from the cylinder; no length scale information was reported for this turbulence. The experiment reported that the separation and the wake were periodic although there was some modulation of the periodicity. In addition to time-averaged quantities, the experiment reported a number of phase-averaged quantities at various locations in the flow. Selected experimental measurements of this flow will be presented below along with the simulation results.

The geometry of the flow and the corresponding parameters, including the overall domain size specified to the participants, are given in Fig. 1 and Table 1, respectively. Other than the inflow conditions, the computors were asked to apply the following conditions:

- Slip (symmetry) conditions at the lateral boundaries. The lateral size of the domain was provided in order to eliminate one variable; its value is given in Table 1.
- A choice of zero gradient or convective boundary conditions at the downstream boundary. In fact, convective conditions were used exclusively.
- A choice of no-slip boundary conditions or wall functions at the cylinder surface. All participants chose to use wall functions.

The second flow selected (designated Case B) was the flow over a cube mounted on one wall of a channel flow for which the measurements were taken from the work of Martinuzzi (1992) and Martinuzzi and Tropea (1993). The Reynolds number is 40,000 and the upstream flow is fully developed channel flow. The geometry and parameters, including the domain specifications, for this case are given in Fig. 2 and Table 2, respectively. This flow is fully turbulent everywhere and displays no obvious regularity or periodicity.

Other than fully developed channel flow at the inlet, the computors were asked to use the following conditions:

Table 1 Dimensions of the calculation domain for the square cylinder flow (Test Case A)

x_1/D	x_2/D	y_1/D	z_1/D
4.5	≥15.0	14.0	4.0

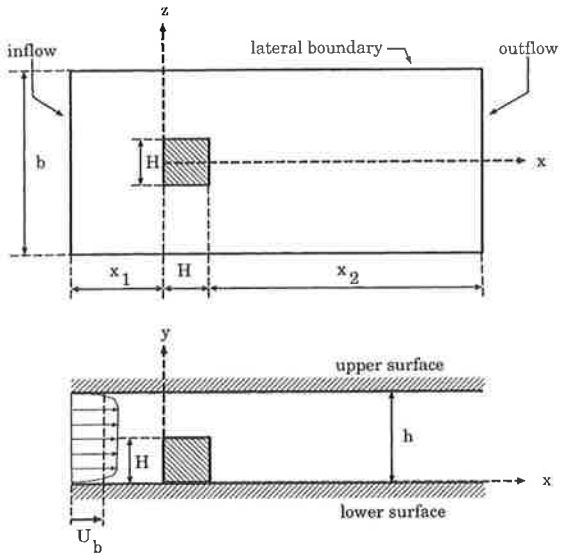

Fig. 2 The geometry of the wall-mounted cube flow (Test Case B) indicating the definitions of the various geometric lengths

- The lateral boundaries were to be treated either as slip surfaces or as periodic boundaries. The width of the domain is given in Table 2.
- A choice of zero gradient or convective boundary conditions at the downstream boundary. As in Case A, convective conditions were used exclusively.
- A choice of no-slip boundary conditions or wall functions at the cylinder surface.

Finally, in order to attempt to assess the effect of Reynolds number on the quality of an LES, a third case was added. This is the cube flow with the parameters given above but at Reynolds number 3000. This case was called B1; the high Reynolds number case was called B2. No experimental data exist for case B1.

The computors were requested to submit data to the organizers prior to the workshop in formats that were provided. Selected data were put into graphical form and given to the attendees when they registered for the meeting. Certain overall parameters (reported below) were also computed by the organizers from the provided data. The participants presented their methods but not their data at the workshop. The data presentations were made by rapporteurs, who are two of the authors of this paper (MB and MP).

5 Computational Methods

As noted, the flows chosen were ones for which Cartesian coordinate systems could be used. This was done so that grids could be generated easily. Despite this, a number of different kinds of grids were used in the calculation.

Most people used Cartesian grids; of these, most employed grid stretching but a few used uniform grids. One computor (Tamura) used two rather unusual grids for Test Case A. The first was an *O*-grid in which one set of coordinate lines encircle the cylinder. The second grid was a uniform Cartesian grid but four levels of refined grids were embedded in the main grid, principally near the surface; these grids were preselected and not created adaptively. Another group (EDF) used a finite element method on a grid consisting of triangular prisms. In all cases, the number of grid points in the spanwise direction (along the cylinder axis) was much smaller than the number employed in the other two directions.

Table 2 Size of the calculation domain for the wall-mounted cube flow (Test Case B)

x_1/H	x_2/H	h/H	b/H
3	≥6	2	7

The most popular discretization method was the finite volume approach; as noted above, there was one finite element submission. Many used second order central difference approximations but some people used upwind methods; among the latter were QUICK and several third order methods.

For time advancement, the most popular method was the second order Adams-Bashforth scheme, but the Runge-Kutta, Euler, and leapfrog methods were used by some.

For the conditions at the surfaces, for Case A, about equal numbers of people used no-slip and wall functions or approximate boundary conditions; the latter were all based on the model of Werner and Wengle (1989). Although the inlet conditions for this case were specified to contain 2 percent turbulence, everyone used uniform laminar inflow conditions; the effect of this modification is difficult to assess as we note below. At the outlet, everyone used convective conditions.

For Case B1, almost everyone used similar methods—control volume methods with second-order approximations, no-slip boundary conditions, and convective outflow conditions. One unusual case used periodic boundary conditions in the streamwise direction. Two of the calculations used wall functions; the others used no-slip conditions. Other major differences are found in the subgrid scale models; the Smagorinsky, mixed, Schumann, and dynamic models were used by various computors.

The methods used in Case B2 were similar to the ones used in Case B1 but everyone applied wall functions at the surfaces.

Some of the details of the computational methods used in the simulations are given in Tables 3, 5, and 6. Computors were asked to provide a large amount of time-averaged and in Case A also phase-averaged statistical data in specified formats. Only the limited amount of results required to illustrate certain points will be included in this paper. It is the feeling of the authors that the detailed descriptions of the results belong to the authors and should be presented in their own papers.

6 Results for Case A and Their Assessment

We note again that Case A is the flow over a square cylinder. A list of submissions and the parameters and methods used is given in Table 3. Ten groups submitted a total of sixteen sets of results. As noted above, detailed discussion of the physics of these flows is reserved to papers by individual contributors.

The contributors were asked to submit the time-averaged velocity field as well as phase-averaged quantities at five different phases. This was more data than the organizers (the authors of the present paper) were able to plot so only partial results were plotted to provide the basis for discussion at the workshop. Obviously, only a much smaller selection can be presented here. Of the results, two clearly differed from the others and the experiments by so much that they were excluded from discussion (TUDELFT, EDF-FE2). Insofar as we are able to determine, the lack of quality in these results apparently derives from insufficient grid near the walls in one case and too little averaging time in the other.

An impression of the nature of the flow can be obtained from the phase-averaged streamline pictures taken from selected calculations shown in Fig. 3. The experimental streamline picture is also included. The shedding motion is qualitatively well predicted, but there are significant quantitative differences among the various calculations and with the experiment. Unfortunately, the region near the cylinder walls is not resolved in the measurements, so the computed flow behavior in this region, which contains a number of vortices, cannot be assessed.

Some important overall parameters of the flow submitted by the contributors as well as the available experimental results

Table 3 Submissions for Case A: groups, parameters and methods

Contrib./Key	Group, Affiliation	Grid	Time Scheme	Convection Scheme	Subgrid-Scale Model	C_s	Wall Damping: (a,b)	Wall Bound. Cond.	$T_{transflow}$	# of cycles
KAWAMU	H. Kawamura, N. Kawashima, Science Univ. of Tokyo, Japan	FD: 128x78x20	AB	Upwind (3rd)	–	–	–	no slip	0%	≈ 4
UMIST1	F. Archambeau, D. Laurence, EDF/LNH	FV: 140x81x13	AB	Central (2nd)	Smagorinsky	0.15	VDD: (1.,1.)	WF	0%	7.5
UMIST2	Chatou, France &	FV: 140x81x13	AB	Central (2nd)	Dynamic	–	–	WF	0%	4
UMIST3	M.A. Leschziner, UMIST, Manchester, U.K.	FV: 140x81x13	AB	Central (2nd)	Dynamic	–	–	WF	0%	7
ILLINOIS1	G. Wang, S.P. Vanka, Univ. of Illinois at Urbana-Champaign, U.S.A.	FV: 144x128x32	AB	QUICK	Dynamic	–	–	no slip	0%	30
ILLINOIS2		FV: 176x144x32	AB	QUICK	Dynamic	–	–	no slip	0%	25
UKAHY1	M. Pourquie, M. Breuer, W. Rodi, Univ. of Karlsruhe/Inst. for Hydromechanics, Germany	FV: 100x105x20	AB	Central (2nd)	Smagorinsky	0.1	VDD: (3.,0.5)	WF	0%	13
UKAHY2		FV: 146x146x20	AB	Central (2nd)	Smagorinsky	0.1	VDD: (3.,0.5)	WF	0%	8
EDF-FE1	P. Miet, D. Laurence, B. Nitrosso, EDF/LNH, Chatou, France	FE: 76159	OS	Charact. M.	Smagorinsky	0.2	VDD: (1.,1.)	WF	0%	≈ 10
EDF-FE2		FE: 113856	OS	Charact. M.	Smagorinsky	0.065	VDD: (1.,1.)	WF	0%	7
TAMU1	T. Tamura, Y. Itoh, A. Takakuwa, Tokyo Inst. of Technology, Japan	FV: 202x100x102	EU	Upwind (3rd)	no	–	–	no slip	0%	9
TAMU2		FV: 165x113x17	EU	Upwind (3rd)	Dynamic	–	–	no slip / WF	0%	6
ONERA	K. Dang-Tran, P. Sagaut, ONERA, Chatillon, France	FV: 231x125x21	EU	mixed FE/FV	Mixed Scale	–	–	no slip	0%	8
TUDELFT	B.J. Boersma, L.J.P. Timmermans, F.T.M. Nieuwstadt, Delft Univ. of Technology, The Netherlands	FV: 274x260x50	RK	Central (2nd)	Smagorinsky	0.17	VDD: (?,?)	no slip	RG: 2%	15
IIS-KOBA	T. Kobayashi, N. Taniguchi, T. Kogaki, Inst. of Indust. Science, Univ. of Tokyo, Japan	FV: 83x63x16	AB/CN	QUICK	Smagorinsky	0.13	VDD: (1.,1.)	no slip	RG: 1%	12
IIS-MURA	S. Murakami, S. Iizuka, Inst. of Indust. Science, Univ. of Tokyo, A. Mochida, Y. Tominaga, Niigata Inst. of Technology, Japan	FV: 100x92x22	AB/CN	Central (2nd)	Dynamic Mixed	–	–	WF	0%	≈ 3

AB = Adams-Bashforth (2nd), CN = Crank-Nicolson, EU = Euler Scheme (1st) FD = Finite Difference, FV = Finite Volume, FE = Finite Element
OS = Operator Splitting, RG = Random Generator, RK = Runge-Kutta (2nd), VDD = Van Driest Damping: $(1-exp(-y^+/25)^a)^b)$, WF = Wall Function

for them and RANS results to be discussed later, are given in Table 4. All submittors reported that their computed flows were periodic. We note that, with one or two exceptions, the reported values of the Strouhal number fall in a narrow range close to the experimental value. Apparently, this quantity (and others mentioned later) are not very sensitive to the parameters of the simulation. Among other things, this means that accurate prediction of the Strouhal number is not necessarily an indication of a quality simulation. This is a point to be borne in mind by future authors and reviewers. The former should present results for quantities that are hard to compute accurately; the latter should take care to determine that the simulation has been challenged sufficiently.

The results for the mean drag coefficient shown in the table display considerably more variation than do the Strouhal number results. In fact, several of the results differ by more than 20 percent from the experimental result. It appears that, in general, the simulations that used wall functions produced drag coefficients that are relatively close to the experiments while those that used no-slip conditions tend to produce high values of the drag coefficient. Possible reasons for this observation are given below.

The results for l_r, the length of the time-mean recirculation zone behind the cylinder show even greater variation, with the simulations based on no-slip boundary conditions tending to give smaller values. This is consistent with the drag coefficient results; both sets of results are consistent with the no-slip simulations having lower pressure in the base region behind the cylinder. Better values of l_r seem to be obtained in simulations with greater resolution near the surface, a point that we shall return to below.

The simulations that used wall functions had larger negative velocities close to the side walls of the cylinder; we must assume that this is a direct effect of the application of the wall functions. This increased reversed flow causes the pressure to be higher near the upstream corner so that the flow leaves the corner at a larger angle. In turn, this results in a larger recirculation region. This is an example of how all the results are tied together in this flow. Proper prediction of the wake depends very sensitively on the treatment of the flow near the cylinder.

The fluctuating side force coefficient, $c_{l,rms}$ shows more variation from simulation to simulation than any other result in the table. In general, it appears that simulations that used wall functions tended to predict lower values of these fluctuations.

Selected results for the mean velocity on the center plane of the cylinder are shown in Fig. 4; these were chosen to show the range of the results and the names of the contributors is not important. The experiment shows (somewhat surprisingly) that the velocity recovers for a while and then nearly levels off at about $0.6U_{in}$, where U_{in} is the inlet velocity. Some of the computed results show stronger recovery of the velocity than the experiment, including one that levels off and another that continues to rise. A few were low and one, a simulation by Tamura, displays nearly correct behavior although the recirculation region is a bit short.

Figure 5 shows results for the phase-averaged vertical velocity on the center plane for a particular phase; the results came from the same authors whose results were used in Fig. 4. It is clear that the agreement with each other and with the experiment is better than for the drag coefficient i.e. that this quantity and, indeed, most results concerning the vertical component of the velocity are reasonably well predicted in all simulations. We are unable to offer an explanation for this behavior but it means that the vertical velocity should not be used as a definitive indicator of the quality of a simulation.

In Fig. 6, we present the averaged pressure distribution around the cylinder along with the experimental results of Lee (1975) and Bearman and Obasaju (1982). The pressure on the upstream face is fairly well predicted but the values on the other faces show significant disagreement both with each other and with the experiments, as might be expected from the results for the separation regions. Note, too, the difference in the two sets of experimental results and oscillations in the computed results that probably indicate lack of sufficient resolution.

Finally, in Fig. 7, we show a close-up of the time-averaged streamwise velocity. The point of presenting this figure is not directly connected with the quantity plotted. Rather, it is to show that the grid distribution near the body is insufficient to resolve the region of reversed flow near the wall in most of the simulations. The maximum negative streamwise velocity occurs at the first grid point from the wall in a number of the simulations; this is a definite indicator of insufficient resolution and may explain some of the other observations. The occurrence of the maximum negative velocity at the first grid point indicates that that thickness of the reversed flow region is determined by the grid and not by the physics. More grid points should be employed in this region whether no-slip or wall-function boundary conditions are used.

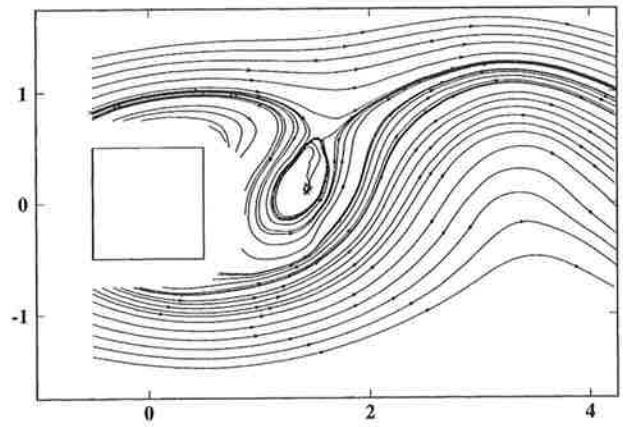

Fig. 3(*a*)

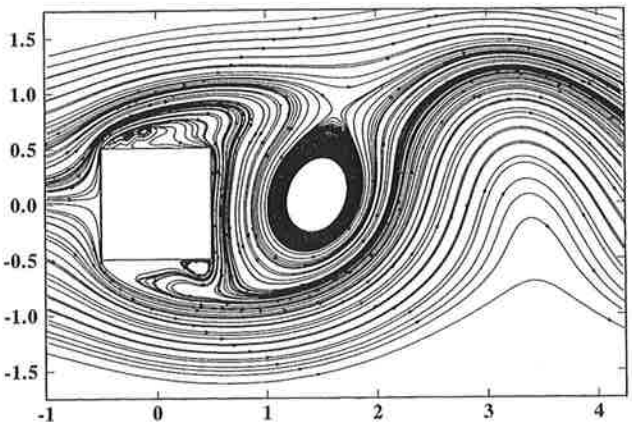

Fig. 3(*b*)

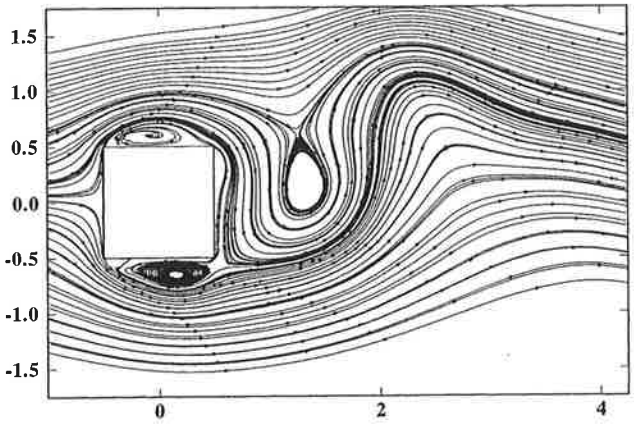

Fig. 3(*c*)

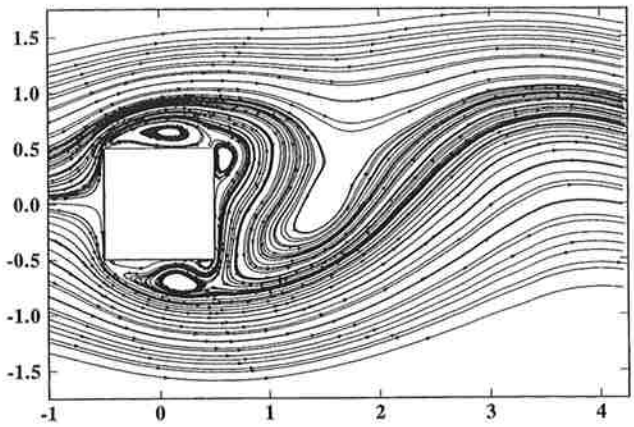

Fig. 3(*d*)

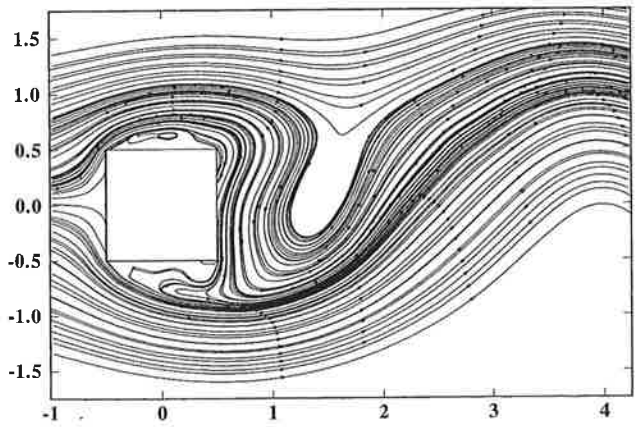

Fig. 3(*e*)

Fig. 3 Phase-averaged streamlines (Phase 01) from several simulations. Figure 3(*a*) is taken from the experiment.

It is important to recall that the inflow to the computational domain is laminar and that transition takes place in the separated shear layers on the sides of the cylinder just downstream of the front corners; this is shown by the experiments (Lyn and Rodi, 1994). It is clear that the resolution in this region (which extends some distance from the body) is not good enough to accurately capture the development and transition of the separated shear layer. Further, given the short length of travel of the reversed flow on the cylinder sides, it is certain that the reversed flows along the side walls are not fully developed turbulent boundary layers. The latter is the type of flow for which the wall functions were designed so the validity of these functions is questionable in the reverse flow regions. However, the instantaneous velocity distribution assumed in the Werner-Wengle near-wall model may be more realistic than the linear distribution assumed when no-slip conditions are used, and this may be part of the reason why using this model leads to better prediction of the drag coefficient. The best treatment would be to the use a sufficiently fine grid to resolve the near-wall flow with no-slip conditions, but this is very expensive and no one was able to perform such a simulation. It is possible that an embedded grid similar to the one used by Tamura could do the job but not enough results are available to allow one to reach a definitive conclusion on this point.

Overall, it is our judgement that no single simulation is uniformly good; significant faults can be found in every submission. It does appear, however, that one key to success is having sufficient resolution near the surface. Without it, the separated regions on the sides of the cylinder (see Fig. 3) cannot be correctly predicted and are unlikely to have the correct average thickness. This, in turn, affects the pressure distribution on the body and the size of the recirculation zone. It may also have an important effect on the velocity recovery downstream but it is difficult to address this issue on the basis of the available results.

One of the factors whose effect proved very difficult to analyze is the choice of numerical method. As already noted, a number of computors used upwind methods. Third order upwind methods create a dissipative fourth order error term that acts like an additional subgrid scale model. The QUICK scheme is similar. The simulations that used these methods tended to predict short recirculation zones; it is likely that the shortening of the recirculation zone is due, at least in part, to the diffusion added by the numerical approximation. In order to assess this, it would be useful to know the dissipation created by the numerical method; unfortunately, it was not computed and is not avail-

Table 4 Bulk coefficients for Case A

Contribution	$\overline{c_l}$	$c_{l,rms}$	$\overline{c_d}$	$c_{d,rms}$	St *	l_r
EDF-FE1	0.03	0.73	1.86	0.12	0.13	1.65
EDF-FE2	0.007	0.38	1.66	0.10	0.066	1.33
IIS-KOBA	-0.3	1.31	2.04	0.26	0.13	1.22
IIS-MURA	-	-	2.06	0.13	-	1.26
ILLINOIS1	-0.03	1.38	2.67	0.24	0.13	0.89
ILLINOIS2	-0.02	1.40	2.52	0.27	0.13	0.95
KAWAMU	-0.005	1.33	2.58	0.27	0.15	1.2
ONERA	-0.01	0.65	2.01	0.18	0.11	1.12
TUDELFT	-	-	1.96	-	0.14	2.96
UKAHY1	-0.02	1.01	2.20	0.14	0.13	1.32
UKAHY2	-0.04	1.15	2.30	0.14	0.13	1.46
UMIST1	0.	-	2.39	-	0.125	0.91
UMIST2	0.	-	2.02	-	0.09	1.21
UMIST3	0.	-	1.93	-	0.137	1.28
TAMU1	-0.03	1.37	2.28	0.20	0.13	1.15
TAMU2	-0.09	1.79	2.77	0.19	0.14	0.94
RANS results						
Bosch (1995)						
standard k–ϵ	-	-	1.637	-	0.134	2.84
KL modification	-	-	1.789	-	0.142	2.04
two-layer k–ϵ	-	-	1.719	-	0.137	2.42
two-layer with KL model	-	-	2.004	-	0.143	1.25
Franke & Rodi (1993)						
RSE model	-	-	2.150	-	0.136	0.98
two-layer RSE	-	-	2.430	-	0.159	0.98
Experiments						
Lee (1975)			2.05	0.16-0.23	-	
Vickery (1975)		0.68-1.32 *	2.05		-	
Cheng et al. (1992)		0.1-0.6 *	1.9-2.1	0.1-0.2 *	-	
McLean et al. (1992)		0.7-1.4 *	1.9-2.1	0.1-0.2 *	-	
Lyn et al. (1994, 1995)		-	2.1	- -	0.132	1.38

*: Strouhal number estimated from peak in lift spectrum
*: variation with degree of incoming turbulence (0 – 10%) and length scale of incoming turbulence

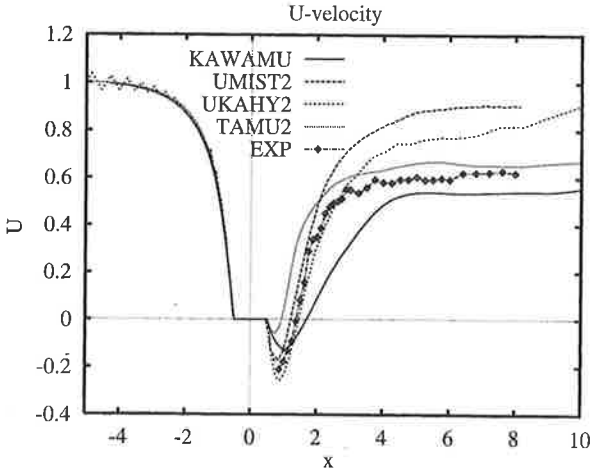

Fig. 4 The mean velocity distribution on the center plane of the cylinder from several simulations chosen to show the range of the results

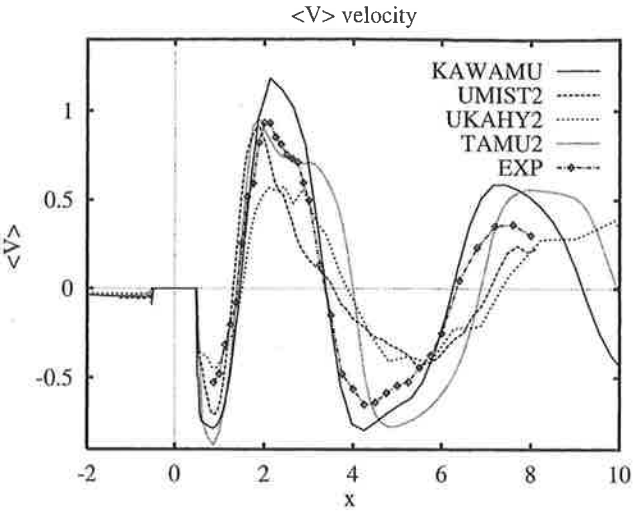

Fig. 5 The phase-averaged vertical velocity distribution (for Phase 01) on the center plane of the cylinder from the same set of simulations as in Fig. 4

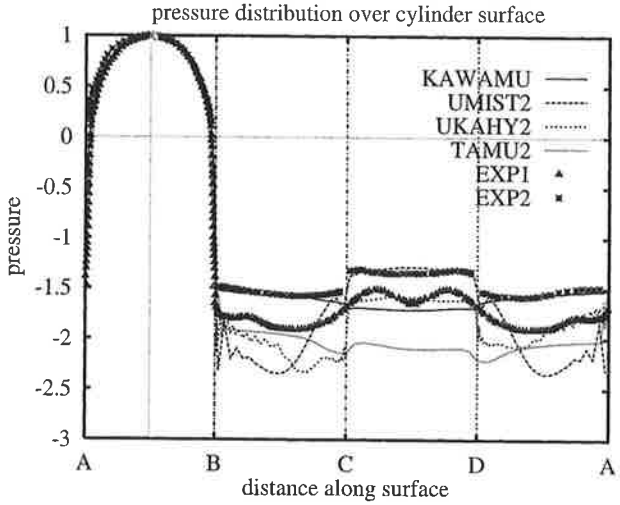

Fig. 6 The average pressure on the body from the same set of simulations as in Fig. 4 and the experimental results of Lee (1975) and Bearman and Obasaju (1982)

able to us. It should be presented in any paper based on upwind methods and any future workshop of this type.

It appears that the simulations that used the dynamic model tended to predict longer recirculation zones and lower drag coefficients than those that used the Smagorinsky model. A figure presenting the distribution of eddy viscosity produced by the two models that was shown at the meeting indicates that the dynamic model produces a larger eddy viscosity than the Smagorinsky model in the shear layers and a smaller one almost everywhere else. This is the probably cause of the differences mentioned above. Figure 8 shows the distribution of the spanwise averaged C values computed by the dynamic model at two different instants; this is equivalent to C_s^2 of the Smagorinsky model. In the shear layers, large values of C_s^2 (of the order of 1) appear, whereas low or even negative values are observed in the other regions of the flow. In the simulations, negative values of C_s^2 were clipped by most people in order not to destabilize the numerical algorithm. It is also worth pointing out that the values of the parameter used in the simulations based on the Smagorinsky model are rather large for shear flows; most channel flow calculations have used $C_s = 0.06 - 0.10$. The larger values may be, in part, compensation for the use of the grid size as the filter width rather that the $2\Delta x$ that is widely regarded as more appropriate. This may explain some of the results found with this model.

It is also important to note that nearly all of the simulations used relatively few grid points in the spanwise (cylinder axis) direction; the spanwise extent of the domain was also quite short in most cases. Both of these factors limit the ability of the shear layers to become three dimensional. It is known from the literature that purely two dimensional simulations, for exam-

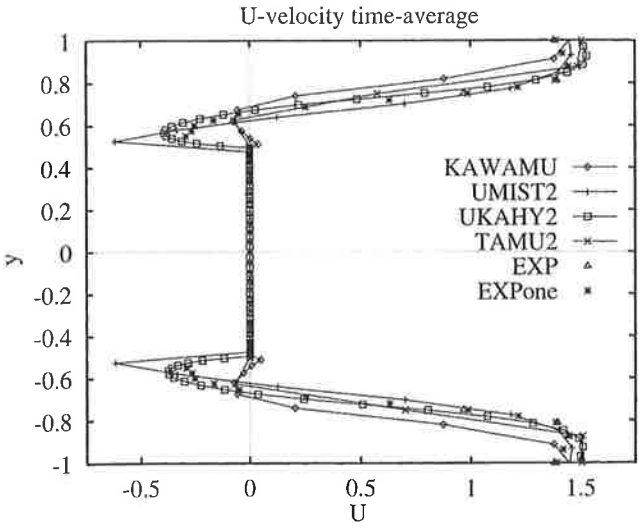

Fig. 7 Close-up of the time-averaged streamwise velocity near the body from the same set of simulations as in Fig. 4

ple, those based on vortex methods, give recirculation zones that are much too long and drag coefficients that are much too small. The experiment shows that the flow is turbulent and therefore three dimensional. Thus this factor may be another contributor to the lack of agreement with experiment demonstrated above.

To sum up, we repeat that none of the simulations was completely satisfactory. Some of the reasons for the lack of agreement with experiment are (not necessarily in order of importance): insufficient resolution near the surface, lack of turbulence in the incoming stream, numerical diffusion, insufficient grid in the spanwise direction, and insufficient width in the spanwise direction. It may be that this flow is very sensitive to small changes in various parameters (this is suggested by the variation in the experimental results). This conjecture should be verified either experimentally or by a careful series of simulations and, if true, it means that this was probably not an ideal choice for a test case.

The evaluation committee, which consisted of J. H. Ferziger, P. Moin, S. P. Vanka, and P. R. Voke, found that the results most useful in helping to discern the effects of the various factors on the simulated flow were those cases in which a single group did more than one calculation. The cases provided by a single group usually modified only a single factor (grid, model, etc.). This allowed conclusions to be drawn about the effect of those factors. It is strongly recommended that the organizers of future meetings of this type commission particular groups to make studies in which only a single factor is modified. Many authors traditionally present only their best results in published papers. Including results obtained with other methods or parameter values (or at least describing them) would be a valuable service and should be encouraged.

It appears that the square cylinder flow is difficult to simulate in part because the inflow is basically laminar and transition takes place in the separated free shear layers on the sides of the cylinder. As suggested above, it may also be sensitive to small changes in various factors. Transitional flows are generally known to be sensitive to minor perturbations, making them difficult to simulate accurately.

7 Results for Case B and Their Assessment

We recall that Case B is the flow over a cube mounted on a wall of a channel. There are two subcases, designated B1 and B2, that have Reynolds numbers 3000 and 40,000, respectively. Four groups provided five submissions for Case B1; three groups provided four submissions for Case B2. Three of the submissions for Case B1 used no-slip boundary conditions; all of the other simulations of both cases used law of the wall type boundary conditions.

Computors were asked to provide the mean velocity field on the center plane of the flow, on a plane just above the wall to which the cube is attached, and near the surfaces of the cube and turbulence data on the center plane; from these data, streamline plots were generated. Participants were also asked for vertical profiles of various quantities at a number of locations.

This flow is not periodic but does contain a considerable amount of coherent structure, at least in the low Reynolds number case. The computors were not asked to provide any data that would permit deduction of coherent structures.

In general, the results for this flow were in better agreement with each other and with the experiments than those for Case A. This is probably due, at least in part, to the fact that the flow is everywhere fully turbulent. The similarity of the numerical methods may be another factor contributing to the agreement among the methods. The results for the two sub-cases will be presented separately.

7.1 Case B1. For Case B1, all but one of the simulations used results taken from a channel flow simulation to provide the inlet conditions. The last used periodic conditions with a period of 21 cube heights in the streamwise direction; the velocity profiles upstream of the cube in this simulation show that

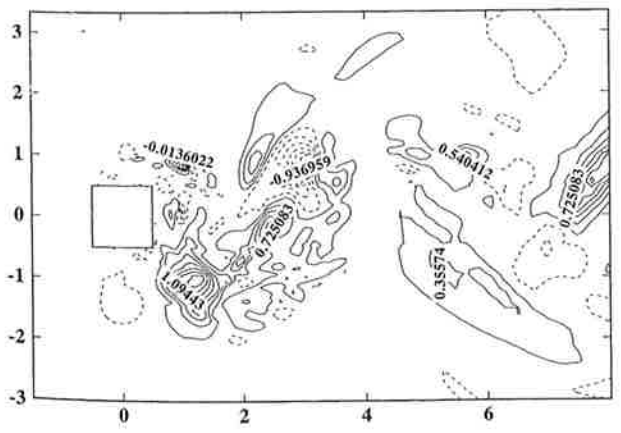

Fig. 8(a)

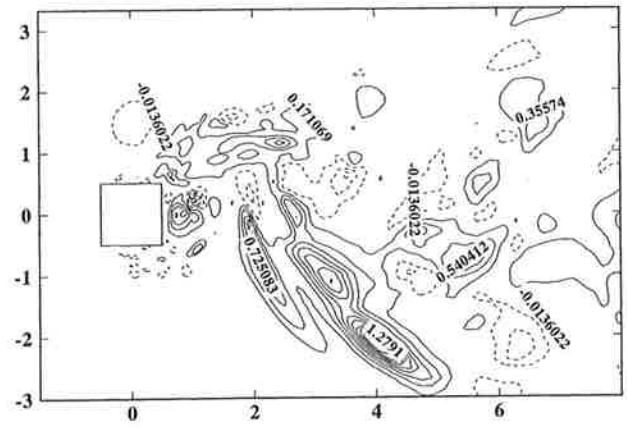

Fig. 8(b)

Fig. 8 Distribution of $C = C_s^2$; values computed by the dynamic model at two different instants, spanwise averaged values, (courtesy of S. P. Vanka, Illinois)

Table 5 Submissions for Case B1: groups, parameters and methods

Contrib./Key	Group, Affiliation	Grid	Time Scheme	Convection Scheme	Subgrid-Scale Model	C_s	Wall Damping: (a,b)	Wall Bound. Cond.	$T_{averaging}$
STANF	K. Shah, J.H. Ferziger, Stanford University, U.S.A.	FV: 128x64x64	CN/RK	Central (2nd)	Dynamic Mixed	–	–	no slip	75
UKAHY1	M. Breuer, M. Pourquie, W. Rodi, Univ. of Karlsruhe, Inst. for Hydromechanics, Germany	FV: 165x65x97	AB	Central (2nd)	Smagorinsky	0.1	VDD: (3.,0.5)	no slip	≈ 103.5
UKAHY2		FV: 165x65x97	AB	Central (2nd)	Dynamic	–	–	no slip	≈ 200.5
UBWM1	H. Wengle, Univ. der Bundeswehr München, Germany	FV: 144x58x88	LF	Central (2nd)	Smagorinsky	0.1	no	WF	750/500
UKAST1	W. Frank, S. Kellmann, Univ. of Karlsruhe/Inst. for Fluid Mechanics, Germany	FV: 240x120x40	EU/LF	Central (2nd)	Schumann	?	?	WF (periodic b.c. in streamwise direction)	?

AB = Adams-Bashforth (2nd), CN = Crank-Nicolson, EU = Euler Scheme (1st) FV = Finite Volume, LF = Leap-Frog
RK = Runge-Kutta (2nd), VDD = Van Driest Damping: $(1 - exp(-y^+/25)^a)^b$), WF = Wall Function

the flow is not able to recover to a fully developed channel flow state in that distance, causing the flow approaching the cube to be different from that in the other simulations. Thus, although it is bothersome to do so, it is best to do simulations with turbulent inflows with inlet conditions taken from other simulations. This submission the used periodic conditions yielded results that were noticeably different from the others and will not be discussed further. Parameters of the submitted simulations are given in Table 5.

It is unfortunate that no experimental data are available at this Reynolds number. However, the considerable similarity of the results for this flow and those for Case B2 and the agreement among the results make it reasonable to conclude that the simulations are probably fairly accurate.

Figure 9 defines the length scales that are presented in Table 7. From the table, we see that there is quite good agreement among the results; they are also quite similar to the results for Case B2 presented in Table 8 below. The major discrepancy among the results is that one simulation predicts mean flow reattachment on the roof of the cube while the others do not. In the absence of experimental data it is impossible to say with certainty which prediction is correct. However, the participant who found reattachment in this case also finds it in Case B2 and the participant who did not find reattachment and also computed Case B2 did not find it in either case. The high Reynolds number experiment showed no reattachment; from this one can infer that mean reattachment should not occur on the roof of the cube.

Note, too, that in the two simulations done by the same group, the only difference was the choice of subgrid scale model. The dynamic model produces smaller values of all the length scales presented in Table 7. The other calculation that used a dynamic model gave slightly larger length scales than this simulation; the model in the latter simulation is a modified dynamic model. It is more likely that the differences between these sets of results are due to the differences in the grid.

Figure 10 shows the streamlines of the mean flow on the centerplane of the flow. One can readily identify the heads of the horseshoe and arch vortices (upstream and downstream of the cube, respectively), the recirculation zones in front of and behind the cube that contain these vortices and small secondary separated flow regions in the up- and down-stream corners. A closer view reveals that there are some differences among the predictions with respect to the size and location of these vortices.

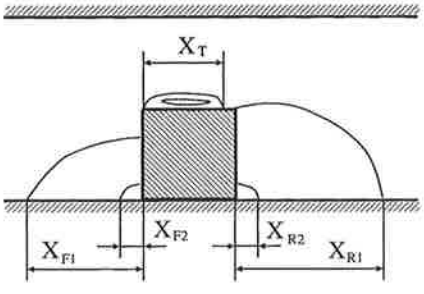

Fig. 9 Definition of length scales in the cube flow

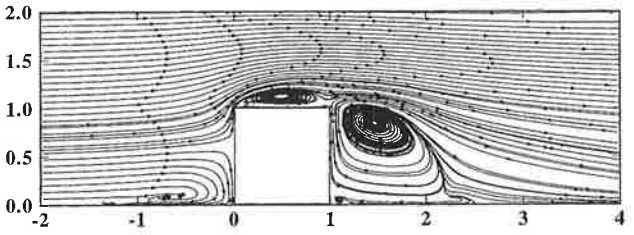

Fig. 10(*a*)

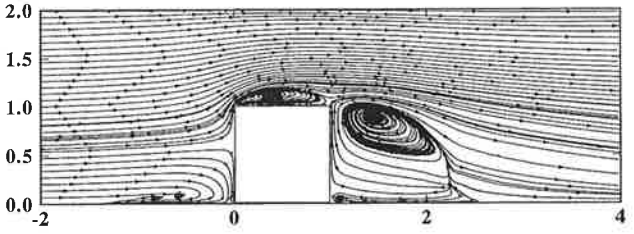

Fig. 10(*b*)

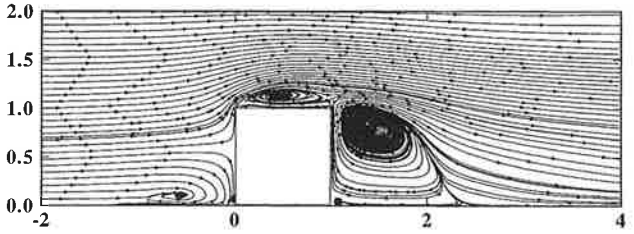

Fig. 10(*c*)

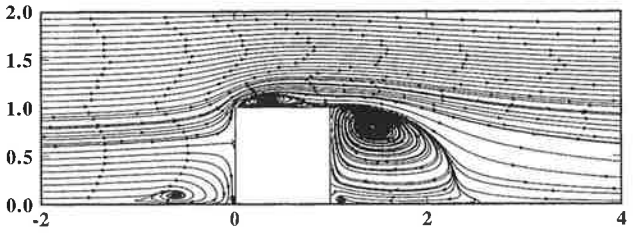

Fig. 10(*d*)

Fig. 10 Streamlines of the mean flow projected onto the centerline of the cube flow of Case B1

The surface streamlines on the floor of the channel are shown in Fig. 11. The lack of symmetry in the right part of the figure is an indication that these simulations have not been run long enough to completely stabilize the statistical averages. Unlike many other flows that have been treated with LES, this one contains almost no statistically equivalent points over which the results can be averaged. (There are equivalent points on the two sides of the symmetry plane of the cube but this hardly provides enough averaging to be worthwhile. Not performing

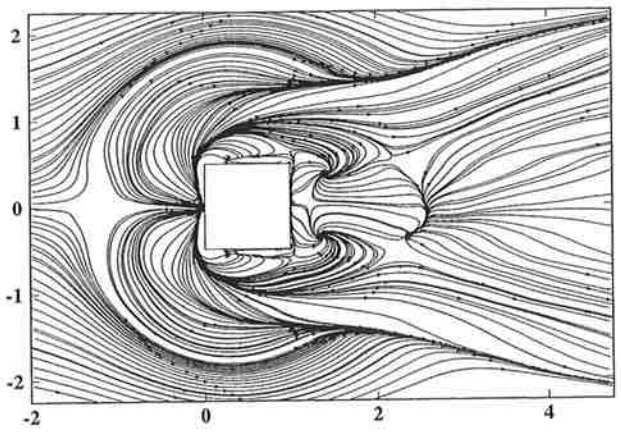

Fig. 11(a)

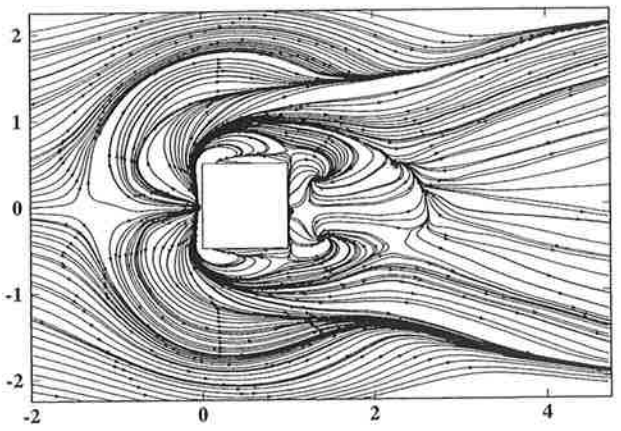

Fig. 11(b)

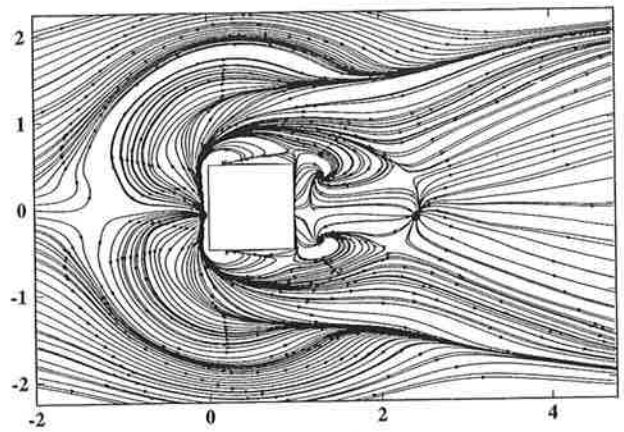

Fig. 11(c)

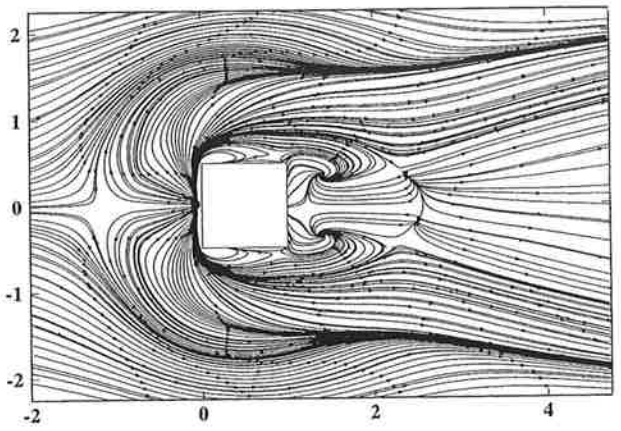

Fig. 11(d)

Fig. 11 Streamlines of the mean flow projected onto the floor of the channel in the cube flow of Case B1

the averaging allows symmetry to provide a measure of whether the simulation has been run long enough.)

In the surface streamline plot, one can discern the footprints of the horseshoe vortex (indicated by converging and diverging streamlines on the sides of the cube) and the arch vortex behind the cube, a forward stagnation point, and the principal reattachment line behind the cube. Some differences in the four figures are found behind the body; most of the other results submitted resemble the left part of the figure more than the right and are not shown for that reason.

The mean velocity profiles upstream of the cube (not shown here) reveal that the simulations have different mean mass fluxes (up to 6 percent variation) on the centerplane even though all cases have the same (specified) total mass flux. This is another consequence of the relatively short averaging time; the averaging times in the simulations varied between 30 and 100 D/U where D is the cube height and U is the bulk velocity at the inlet. Queries to the computors produced the response that the mass fluxes averaged over the inflow plane agreed to within about 1 percent.

The mean velocity profiles above the cube shown in Fig. 12 show no evidence that the grid resolution is causing severe problems. Note that there is also not enough evidence to support the contention that refinement of the grid would not change the results. Indeed, some of the results show small "wiggles" that are probably due to insufficient resolution. The velocity profiles in the recirculation region behind the cube (Fig. 12(b)) show fairly good agreement for a quantity that we had expected to be difficult to compute accurately.

7.2 Case B2. For Case B2, all of the simulations used the results of a channel flow simulation to provide the inlet conditions and used wall functions at the surface. A list of the parameters used in obtaining the simulation results is given in Table 6.

Table 8 gives the length scales of the simulated flows, RANS calculations to be discussed later, and the experimental values. The agreement with each other is quite good but not as good as it was in Case B1. The agreement with the experimental results is also quite good. The length, X_{F1}, locates the upstream stagnation point. Between this point and the cube, there is a very thin region of upstream moving fluid that is difficult to resolve accurately in either the experiment or the simulations so the values should be regarded with more suspicion than those for the other quantities.

For the primary reattachment length, the agreement among the simulations based on the Smagorinsky model is quite good but the one simulation that used the dynamic model, which is identical to the simulation above it in the table in every other way, predicts a shorter reattachment length. This is consistent with what was found in Case B1. Comparison of Tables 7 and 8 shows that the Reynolds number does not seem to affect the length scales (other than the location of the upstream stagnation point) very much.

The streamlines on the center plane of the flow shown in Fig. 13 demonstrate that the agreement with experiment is quite good. The most important differences are found in the head of the horseshoe vortex but this is a region where the experimental uncertainty is relatively large so it is not clear whether the simulations or experiments are more nearly correct.

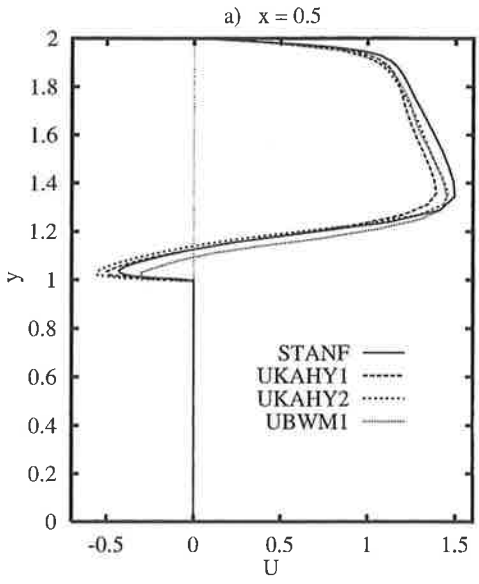

Fig. 12(*a*)

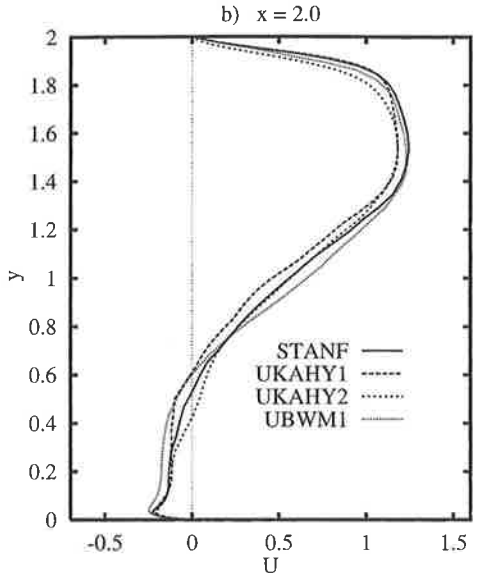

Fig. 12(*b*)

Fig. 12 Profile of the mean streamwise velocity *U* at two different locations in the symmetry plane of the cube, Case B1

Table 6 Submissions for Case B2: groups, parameters and methods

Contrib./Key	Group, Affiliation	Grid	Time Scheme	Convection Scheme	Subgrid-Scale Model	C_s	Wall Damping: (a,b)	Wall Bound. Cond.	$T_{averaging}$
UKAHY3	M. Breuer, M. Pourquie, W. Rodi, Univ. of Karlsruhe,	FV: 165x65x97	AB	Central (2nd)	Smagorinsky	0.1	VDD: (3.,0.5)	WF	≈ 150.1
UKAHY4	Inst. for Hydromechanics, Germany	FV: 165x65x97	AB	Central (2nd)	Dynamic	–	–	WF	≈ 108.6
UBWM2	H. Wengle, Univ. der Bundesnehr München, Germany	FV: 144x58x88	LF	Central (2nd)	Smagorinsky	0.1	no	WF	≈ 700/650
IIS-KOBA	T. Kobayashi, N. Taniguchi, T. Kogaki, Inst. of Industrial Science, Univ. of Tokyo, Japan	FV: 66x36x46	RK	Central (2nd)	Smagorinsky	0.1	VDD: (1.,1.)	WF	10

AB = Adams-Bashforth (2nd), CN = Crank-Nicolson, EU = Euler Scheme (1st) FV = Finite Volume, LF = Leap-Frog
RK = Runge-Kutta (2nd), VDD = Van Driest Damping: $(1-exp(-y^*/25)^3)^{\frac{1}{3}}$, WF = Wall Function

The surface streamlines on the channel floor are shown in Fig. 14 and display all of the features described for Case B1. Indeed, the two cases are so similar that there is not much to add to the discussion given above. Insofar as can be determined (the experimental photograph is somewhat difficult to read), the agreement with experiment is quite good.

Two velocity profiles above and behind the cube are shown in Fig. 15. The agreement with the experimental data is satisfactory but the differences between the computed results are much larger than in Case B1 and some simulations give velocities that are much too small in the reverse-flow region. It is difficult to discern from this plot whether the boundary conditions that were used are satisfactory or not.

The results discussed above, as well as those for Case A, show that, compared to the Smagorinsky model, the dynamic model usually yields larger subgrid scale eddy viscosities in the shear layers surrounding the separated flow zones and smaller eddy viscosities in the recirculation regions themselves. This is reasonable behavior but it is difficult to demonstrate that the dynamic model actually produces better simulations than the Smagorinsky model. It does seem likely, however, since the distribution of the viscosity is more in keeping with expectations, that some version of the dynamic model will ultimately yield superior simulations.

Table 7 Lengths for Case B1; see Fig. 9 for definitions of these length scales

	Separation/Reattachment Length				
Contribution/key	X_{F1}	X_{F2}	X_T	X_{R1}	X_{R2}
STANF	1.31	0.040	—	1.53	0.22
UKAHY1	1.39	0.059	—	1.60	0.24
UKAHY2	1.29	0.072	—	1.42	0.17
UBWM1	1.24	0.058	0.836	1.59	0.22

Table 8 Lengths for Case B2; see Fig. 9 for definitions of these length scales

		Separation/Reattachment Length			
Contribution/key		X_{F1}	X_T	X_{R1}	X_{R2}
EXP (Martinuzzi, 1992) (Martinuzzi and Tropea, 1993)	EXP	1.040	—	1.612	?
LES	UKAHY3	1.287	—	1.696	0.265
	UKAHY4	0.998	—	1.432	0.134
	UBWM2	0.808	0.837	1.722	?
	IIS-KOBA	0.835	0.814	1.652	?
RANS (Breuer et al., 1995)	Standard $k-\varepsilon$	0.651	0.432	2.182	0.021
	KL modification	0.650	—	2.728	0.020
	Two-layer $k-\varepsilon$	0.950	—	2.731	0.252

8 Comparison With RANS Models

Test cases A and B2 have also been calculated with various RANS models by one of the organizer's groups (Franke and Rodi, 1993; Breuer et al., 1995; Bosch, 1995). For case A the unsteady two-dimensional phase-averaged equations were solved, i.e., the periodic motion was resolved, while the effect of the superimposed stochastic turbulent motion was simulated with various turbulence models for the phase-averaged Reynolds stresses. The standard $k-\epsilon$ model, a modification due to

Kato and Launder (1993) which suppresses turbulence production in the stagnation region, and a Reynolds-stress equation (RSE) model by Launder et al. (1975) were employed. In each case, either wall functions or a two-layer approach in which a one-equation model is applied in the near-wall region was used.

The Strouhal number is well predicted by most of the various RANS models, but the Kato-Launder (KL) modification produces values that are somewhat too large and the two-layer RSE model yields an excessive value (see Table 4). The mean drag coefficient is significantly underpredicted by the standard $k - \epsilon$ model, but a roughly correct value is obtained when the KL modification is used with the two-layer approach. The RSE model gives the correct value of $\overline{c_d}$ with wall functions but overpredicts it if the two-layer approach is used. This result is consistent with the significant overprediction of the length of the recirculation region by the standard $k - \epsilon$ model and its underprediction by the two-layer RSE model. There is a severe underprediction of the fluctuating energy in the former case and an overprediction in the latter. The KL modification to the $k - \epsilon$ model in combination with the two-layer approach gives overall the best prediction of the centerline velocity, especially in the near-field, but further downstream the velocity recovers faster than in the experiments. None of the RANS results is close to the measured behavior further downstream, in contrast to at least some of the LES calculations shown in Fig. 4. If plotted on Fig. 5, the best RANS calculations would be as good as the better LES calculations. Although the total fluctuating energy is roughly correct, the stochastic part is severely underpredicted and the periodic part is overpredicted. Hence, while the RANS calculations can certainly be used for practical applications, they are not satisfactory in a more detailed view. On a VP S 600 vector computer, the $k - \epsilon$ model RANS calculations using wall functions took 2 hours and the two-layer calculations 8 hours, compared with 46 hours for the UKAHY1 LES calculations.

Case B2 was calculated with various versions of the $k - \epsilon$ model by Breuer et al. (1995): the standard model and the KL modification using wall functions, and the standard model in a two-layer approach using a one-equation model near the wall. The lengths defined in Fig. 9 predicted with these models are included in Table 8. It can be seen that all the RANS models overpredict the length of the separation zone behind the cube significantly. The standard $k - \epsilon$ model predicts early reattachment of the flow on the roof. Due to suppression of turbulence production in front of the cube, this situation is improved somewhat using the KL modification; the most realistic prediction is, however, obtained with the two-layer approach which resolves the flow on the roof better. This is also the only model in which the near-wall flow structure is close to that shown in Fig. 14; the models that use wall functions do not produce these details. Results are not available for a combination of the KL modification and the two-layer approach, but as with case A, this model version would probably give the best overall prediction (especially in the stagnation, roof, and near-wall regions), but the recirculation region would probably be too long. Hence, the velocity profiles, especially further downstream of the cube, are significantly better predicted by LES, and the turbulence quantities are in significantly better agreement with the experiments. In this case LES shows a clear superiority for which a high price has to be paid: on the VP S 600 the LES calculations (UKAHY4) took 160 hours while the RANS two-layer model calculations took 6 hours and the RANS calculations using wall functions only 15 minutes.

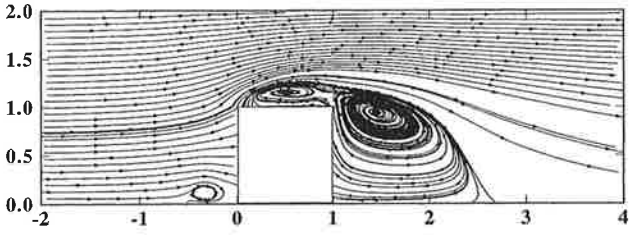

Fig. 13(*a*)

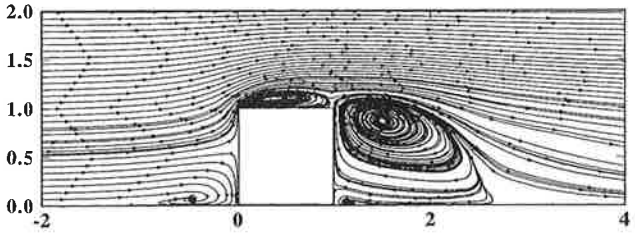

Fig. 13(*b*)

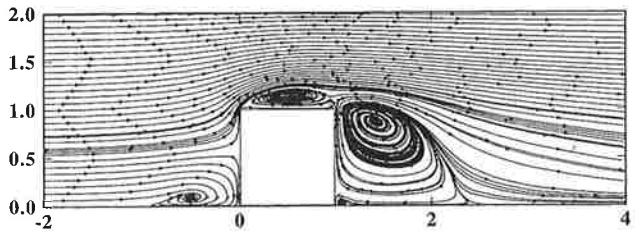

Fig. 13(*c*)

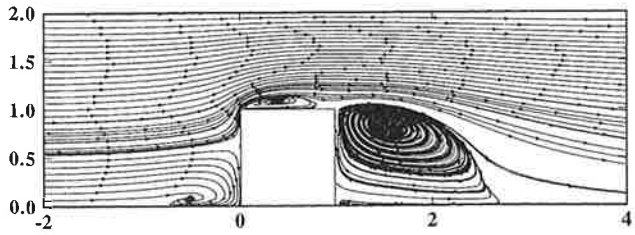

Fig. 13(*d*)

Fig. 13 Streamlines of the mean flow projected onto the centerline of the cube flow of Case B2

9 Conclusions

The results presented above show that LES does not automatically produce excellent results for every flow. To obtain quality results, many factors must be controlled carefully. Included among these are the following:

- *Flow:* Of the cases considered here, the cube flow was predicted much more accurately than the square cylinder flow. It appears that this is a consequence of the square cylinder flow having a transitional character and the possibility (which should be investigated) that this flow is much more sensitive to small changes in the controlling parameters. In general, it appears that transitional flows are more challenging than fully developed ones.
- *Grid:* The results are sensitive to the grid used in the simulation. It is important to resolve those regions of the flow in which the major part of the production of the turbulence and/or transition take place. This may need to be done on a kind of adaptive way in which the grid is changed after simulations are performed. Physical insight into the nature of the flow can be a considerable aid to improving the grid and should be used whenever possible and subject to examination and improvement as suggested above.
- *Boundary Conditions:* 'Law of the wall' boundary conditions can definitely reduce the cost of a simulation by something an order of magnitude. However, they do not seem to be reliable enough to be used with confidence in separated flows. It would be useful to look in detail at the

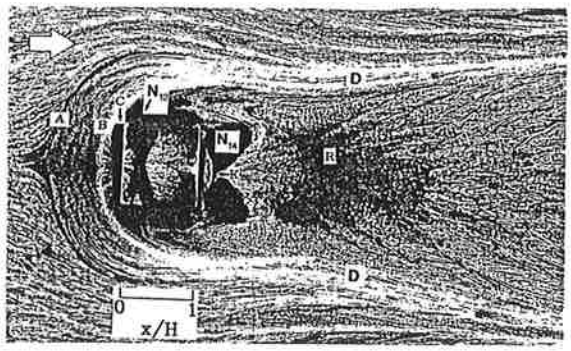

Fig. 14(*a*)

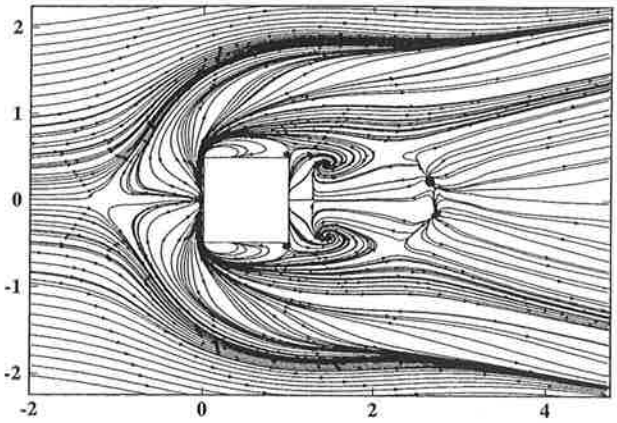

Fig. 14(*b*)

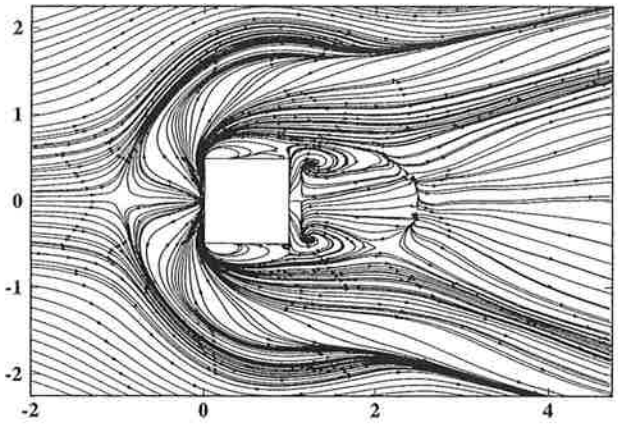

Fig. 14(*c*)

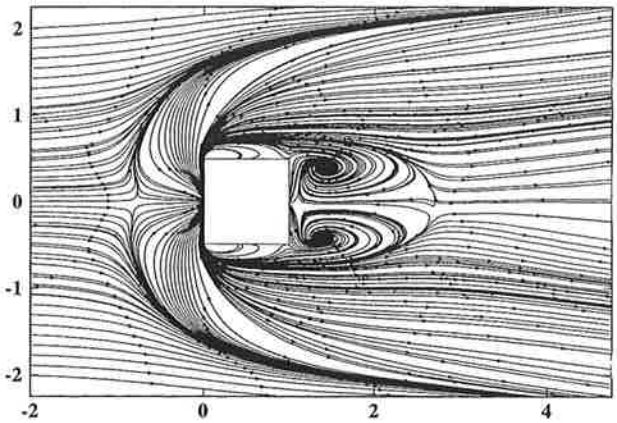

Fig. 14(*d*)

Fig. 14 Streamlines of the mean flow projected onto the floor of the channel in the cube flow of Case B2 along with an experimental oil-flow photograph

near wall region of the cube flow to determine why the high Reynolds number calculations are as good as they are.

- *Subgrid Scale Model:* The predictions produced by different subgrid scale models differ, and, as expected, the differences are larger at high Reynolds number. The dy-

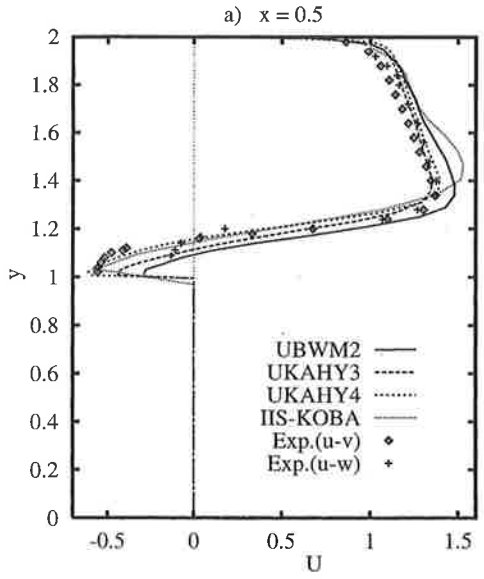

Fig. 15(*a*)

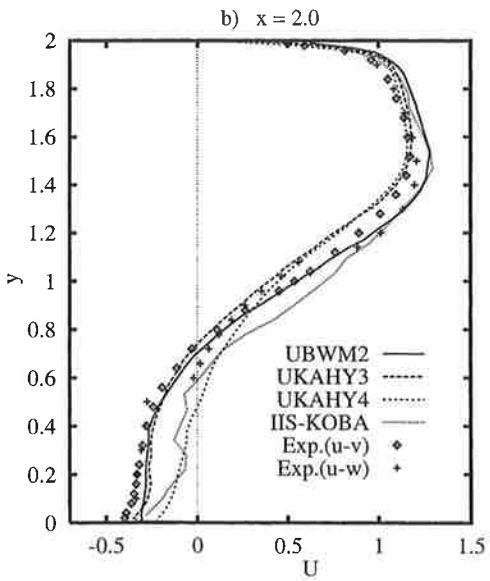

Fig. 15(*b*)

Fig. 15 Profile of the mean streamwise velocity *U* at two different locations in the symmetry plane of the cube, Case B2

namic model appears to produce a better spatial distribution of the subgrid scale eddy viscosity but not necessarily better overall results relative to the Smagorinsky model. We need to understand why that is and how to further improve the models.

- *Numerical Method:* The results produced by different numerical methods with similar grids certainly differ. We need to learn how to estimate the numerical errors and to determine their effects on the results, and, eventually, to learn how to control them.
- *Domain Size:* It is well-known that boundary conditions can affect the solution within a domain if the domain is not large enough. It is possible that the domain specified for the square cylinder flow is too small. There are no indications that this is the case in the cube flow.

10 Recommendations

We anticipate that there will be more workshops of this type in the future. It is natural that, in the course of a workshop of this kind, one learns things that would have made it better. We would therefore like to share some observations and make some final remarks.

Much of what was learned in terms of how the various factors affect the results was gleaned from those cases in which a single group made multiple simulations that differed in just one factor. It is therefore strongly recommended that, in future workshops of this type, one attempts to have all of the groups do one case in which all of the relevant factors are specified, and then ask them to vary one of the factors listed above in a systematic way. This would also be a useful direction for the authors of research papers to follow.

It is probably best to avoid transitional flows as they are difficult to treat with LES. Alternatively, given sufficient interest, it might be possible to have a workshop devoted entirely to this important subject.

It would be very useful to have participants present their values of eddy viscosity (assuming that type of model is used) and the dissipation produced by it. It is also important to require people who use upwind methods to report the dissipation caused by the numerical scheme.

Special attention must be devoted to the regions near solid surfaces. It is clear that many of the difficulties arise in this region. It appears that the boundary conditions intended to allow a simulation to avoid computing the wall region that exist today are not reliable.

Finally, there is a need to tackle still more complex geometries. Performing LES on unstructured grids, while it can certainly be done, still needs to be established. The one finite element submission to this workshop was not polished enough to provide as much information as one would have liked.

It is important that a workshop of this kind not become a contest in which the contributors argue about which simulation is best; the term "Olympics" that has been applied to workshops of this kind in the past is best avoided. The objective should be nothing more or less than to determine what is necessary to do the job well.

Properly chosen RANS models can simulate these flows at lower cost but also at lower accuracy. In flows in which 'significant extra strains' are present and large scale structures dominate the turbulent transport, RANS modeling will be very difficult but there is no reason to expect that LES will not be able to simulate them. Therefore the best opportunities for early application of LES will probably be to flows with complex strains and dominant large scale structures but only moderately complex geometry.

Acknowledgments

The authors are exceedingly grateful to the Max Planck Foundation which provided the primary support for the conference that is the subject of this paper through the Alexander von Humboldt Foundation. Additional support was provided by Electricité de France and Advanced Scientific Computing (Germany) GmbH. We also need to thank the participants in the conference who generously provided their results and, especially, the other members of the evaluation committee: P. Moin, S. P. Vanka, and P. R. Voke.

References

Andren, A., Brown, A. R., Graf, J., Mason, P. J., Moeng, C. H., Nieuwstadt, F. T. M., and Schumann, U., 1994, "Large Eddy Simulation of a Neutrally Stratified Boundary Layer," *Quarterly Journal of the Royal Meteorological Society,* Vol. 120, pp. 1457–1484.

Bardina, J., Ferziger, J. H., and Reynolds, W. C., 1980, "Improved Subgrid Models for Large Eddy Simulation," AIAA paper 80-1357.

Bearman, P. W., and Obasaju, E. D., 1982, "An Experimental Study of Pressure Fluctuations on Fixed and Oscillating Square Section Cylinders," *Journal of Fluid Mechanics,* Vol. 119, pp. 297–321.

Bosch, G., 1995, Experimentelle und theoretische Untersuchung der instationären Strömung um zylindrische Strukturen, Ph.D. Thesis, University of Karlsruhe.

Breuer, M., Lakehal, D., and Rodi, W., 1996, "Flow around a Surface Mounted Cubical Obstacle: Comparison of LES and RANS-Results," IMACS-COST Conference on Computational Fluid Dynamics, Three-Dimensional Complex Flows, Lausanne, Switzerland, Sept. 13–15, (1995), *Computation of 3D Complex Flows,* M. Deville, S. Gavrilakis and I. L. Rhyming, eds., *Notes on Numerical Fluid Mechanics,* Vol. 53, pp. 22–30, Vieweg Verlag, Braunschweig.

Breuer, M., and Pourquie, M., 1996a, "First Experiences with LES of Flows past Bluff Bodies," *Proceedings of the 3rd International Symposium of Engineering Turbulence Modelling and Measurements,* Heraklion-Crete, Greece, May 27–29, 1996, *Engineering Turbulence Modelling and Experiments,* Vol. 3, pp. 177–186, W. Rodi and G. Bergeles, eds., Elsevier Science B.V.

Breuer, M., and Rodi, W., 1996b, "Large-Eddy Simulation of Complex Turbulent Flows of Practical Interest," *Flow Simulation with High-Performance Computers II,* E. H. Hirschel, ed., *Notes on Numerical Fluid Mechanics,* Vol. 52, pp. 258–274, Vieweg Verlag, Braunschweig.

Cheng, C. M., Lu, P. C., and Chen, R. H., 1992, "Wind Loads on Square Cylinder in Homogeneous Turbulent Flows," *Journal of Wind Engineering,* Vol. 41, pp. 739–749.

Clark, R. A., Ferziger, J. H., and Reynolds, W. C., 1979, "Evaluation of Subgrid Scale Turbulence Models Using a Fully Simulated Turbulent Flow," *Journal of Fluid Mechanics,* Vol. 91, pp. 1–16.

Deardorff, J. W., 1970, "A Numerical Study of Three-Dimensional Turbulent Channel Flow at Large Reynolds Number," *Journal of Fluid Mechanics,* Vol. 41, pp. 453–480.

Ferziger, J. H., 1983, "Higher Level Simulations of Turbulent Flow," in: *Computational Methods for Turbulent, Transonic, and Viscous Flows.* J.-A. Essers, ed., Hemisphere.

Ferziger, J. H., 1996, "Large Eddy Simulation," *Simulation and Modeling of Turbulent Flows,* M. Y. Hussaini and T. Gatski, eds., Cambridge University Press.

Franke, R., and Rodi, W., 1993, "Calculation of vortex shedding past a square cylinder with various turbulence models," *Proceedings of 8th Symposium on Turbulent Shear Flows,* F. Durst et al., eds., Springer-Verlag, Berlin, pp. 189–204.

Germano, M., Piomelli, U., Moin, P., and Cabot, W. H., 1991, "A Dynamic Subgrid Scale Eddy Viscosity Model," *Physics of Fluids* A 3 (7), pp. 1760–1765.

Kato, M., and Launder, B. E., 1993, "The modelling of turbulent flow around stationary and vibrating square cylinders," *Proceedings of 9th Symposium on Turbulent Shear Flows,* Kyoto, pp. 10.4.1–10.4.6.

Launder, B. E., Reece, G., and Rodi, W., 1975, "Progress in the development of a Reynolds stress turbulence closure," *Journal of Fluid Mechanics,* Vol. 68, pp. 537–566.

Lee, B. E., 1975, "The Effect of Turbulence on the Surface Pressure Field of Square Prisms," *Journal of Fluid Mechanics,* Vol. 69, pp. 263–282.

Lilly, D. K., 1992, "A Proposed Modification of the Germano Subgrid Scale Closure Method," *Physics of Fluids A,* Vol. 4 (3), pp. 633–635.

Lyn, D. A., and Rodi, W., 1994, "The Flapping Shear Layer Formed by Flow Separation from the Forward Corner of a Square Cylinder," *Journal of Fluid Mechanics,* Vol. 267, pp. 353–376.

Lyn, D. A., Einav, S., Rodi, W., and Park, J.-H., 1995, "A Laser-Doppler-Velocimetry Study of Ensemble-Averaged Characteristics of the Turbulent Near Wake of a Square Cylinder," *Journal of Fluid Mechanics,* Vol. 304, pp. 285–319.

Martinuzzi, R., 1992, "Experimentelle Untersuchung der Umströmung wandgebundener, rechtiger, prismatischer Hindernisse," Ph.D. thesis, University of Erlangen.

Martinuzzi, R., and Tropea, C., 1993, "The Flow around a Surface Mounted Prismatic Obstacle Placed in a Fully Developed Channel Flow," ASME JOURNAL OF FLUIDS ENGINEERING, Vol. 115, pp. 85–92.

Mason, P. J., and Thompson, D. J., 1992, "Stochastic Backscatter in Large Eddy Simulation of Boundary Layers," *Journal of Fluid Mechanics,* Vol. 242, pp. 51–78.

McLean, I., and Gartshore, I., 1992, "Spanwise Correlations of Pressure on a Rigid Square Section Cylinder," *Journal of Wind Engineering,* Vol. 41, pp. 779–808.

Nieuwstadt, F. T. M., Mason, P. J., Moeng, C. H., and Schumann, U., 1992, "Large Eddy Simulation of the Convective Boundary Layer: A Comparison of Four Computer Codes," *Proceedings of 8th Symposium on Turbulent Shear Flows,* F. Durst et al., eds., Springer-Verlag, Berlin, pp. 343–367.

Piomelli, U., Ferziger, J. H., Moin, P., and Kim, J., 1989, "New Approximate Boundary Conditions for Large Eddy Simulations of Wall-Bounded Flows," *Physics of Fluids A,* Vol. 1, pp. 1061–1068.

Rogallo, R. S., and Moin, P., 1994, "Numerical Simulation of Turbulent Flows," *Annual Review of Fluid Mechanics,* Vol. 16, pp. 99–137.

Smagorinsky, J., 1963, "General Circulation Experiments with the Primitive Equations I. The Basic Experiment," *Monthly Weather Review,* Vol. 91, pp. 99–165.

Vickery, B. J., 1975, Fluctuating Lift and Drag on a Long Cylinder of Square Cross Section in a Smooth and a Turbulent Stream," *Journal of Fluid Mechanics,* Vol. 25, pp. 481–494.

Voke, P. R., Kleiser, L., and Chollet, J. P. (eds.), 1994, *Direct and Large Eddy Simulation,* Kluwer Academic Publishers.

Werner, H., and Wengle, H., 1989, "Large Eddy Simulation of Flow over a Square Rib in a Channel," *Proceedings of 7th Symposium on Turbulent Shear Flows,* Stanford University, Aug 21–23, pp. 10.2.1–10.2.6.

(Contents continued)

Technical Briefs

Announcements and Special Notices